This article has been accepted for publication in a future issue of this journal, but has not been fully edited. Content may change prior to final publication. Citation information: DOI 10.1109/JLT.2019.2932844, Journal of Lightwave Technology

Kerr Frequency Comb Generation in Microbottle Resonator with Tunable Zero Dispersion Wavelength

Yiheng Yin, Yanxiong Niu, Haoye Qin, and Ming Ding

***Abstract*—In this paper, we report an optical frequency comb (OFC) generated in a whispering-gallery-mode microbottle resonator, and present a convenient and simple method for adjustment of the zero dispersion wavelength (ZDW). The ZDW tunability of the microbottle resonator realized by exciting modes with different axial mode numbers is predicted theoretically and demonstrated experimentally by changing the coupling position of a tapered fiber. Cascaded four-wave mixing (FWM)-based frequency combs are investigated by pumping the resonator in different dispersion regimes. The results show that the OFC based on degenerated FWM could be generated under the anomalous dispersion, while Raman or Raman-assisted OFC are obtained in the normal dispersion regime.**

***Index Terms*—microresonator, optical frequency comb, ZDW adjustment**

I. Introduction

OPTICAL frequency comb (OFC), which is regarded as a light source with equidistant frequency lines, has been widely employed in many applications, from high-resolution spectroscopy [1], optical frequency metrology [2,3], microwave photonics signal generation [4,5], to fiber telecommunication [6,7]. Recently, whispering-gallery-mode (WGM) microresonators have been experimentally demonstrated as excellent platforms for OFC generation with outstanding theoretical explanations [8-13]. Compared to the OFC based on a mode-locked laser, the WGM-microresonator-based combs, known as Kerr OFC, provide lower threshold powers, larger frequency bandwidths, and more compact integration [9]. The OFC generation process in a WGM microresonator is derived from the parametric-frequency-conversion-induced cascaded four-wave mixing (FWM) [14]. In this process, two pump photons are initially converted to a pair of signal-idler photons, and then the newly generated signal-idler sidebands act as pumps for further parametric frequency conversion [15]. The FWM process occurs when the signal and idler light coincide with the resonator modes, which requires phase matching conditions (momentum conservation and energy conservation) [16,17]. In WGM microresonators, the momentum conservation is satisfied since the propagation constant of a WGM should be expressed as $\beta_m = m/R$, resulting in $2\beta_m = \beta_{m-1} + \beta_{m+1}$ for the signal and idler modes with an equal spacing, where m is the azimuthal mode number and R is the radius of the resonator. However, the energy conservation is determined by the nonequidistant distribution of WGMs owing to the dispersion of the resonator [14]. The zero-dispersion wavelength (ZDW), which represents the wavelength where the dispersion reaches zero, has a decisive role in the process of OFC generation. A broadband frequency comb could be created and a low threshold power is required by pumping the resonator at a wavelength around the ZDW [14]. It is optimal and easier for a microresonator to generate the OFC when the dispersion is in the anomalous regime (the azimuthal free spectral range (FSR_m) increases with the frequency), as the phase matching conditions can be more easily satisfied in this regime [18]. Consequently, the convenient and wide-range adjustment of the ZDW is a significant issue for OFC generation based on a WGM microresonator.

Generally, the adjustment of the WGM microresonator ZDW is realized by changing the structural dimensions. For example, the anomalous dispersion of a solid sphere pumped at a wavelength of λ = 1550 nm appears when the sphere size is larger than 150 μm, while smaller spheres have normal dispersion [19]. For a microtoroid resonator, the ZDW could be adjusted by decreasing the minor toroid diameter [16]. Furthermore, the ZDW of microbubble resonators can be shifted by choosing microresonators with different diameters [20] or wall thicknesses [21-23]. In Ref. [23], a ZDW adjustment range of 0.9 μm was demonstrated by varying the wall thickness in the range of 0.84 to 1.63 μm under a fixed resonator diameter. However, the above ZDW adjustment methods require a high degree of controllability in the fabrication process. Moreover, the geometry parameters of a resonator are fixed after its preparation, except for structure fine tuning by changing the surrounding temperature [24], applying an internal pressure [25], or external tension [26]. However, in this case, a more complex experimental system is required, which is not conducive to practical applications.

In this paper, an OFC generation based on a silica microbottle resonator with an excellent ZDW tunability is reported. The microbottle resonator can sustain a truly three-dimensional (3D) confinement of light, where the WGMs exist not only along the equator of the structure, but also along the axial direction, demonstrating the excellent potentials for dispersion management [27]. Accordingly, in this letter, we

Manuscript received xx xx, 2019; revised xx xx, 2019; accepted xx xx, 2019. Date of publication xx xx, 2019; date of current version xx xx, 2019. This work was supported in part by the National Natural Science Foundation of China under Grant 61575014 (Corresponding author: Ming Ding.)

The authors are with School of Instrumentation Science and Opto - Electronics Engineering , Beihang University, Beijing 100191, China (e -mail: yinyh1987@buaa.edu.cn; niuyx@buaa.edu.cn; qinhaoye@gmail.com; mingding@buaa.edu.cn).

This article has been accepted for publication in a future issue of this journal, but has not been fully edited. Content may change prior to final publication. Citation information: DOI 10.1109/JLT.2019.2932844, Journal of Lightwave Technology

propose a ZDW adjustment method by exciting bottle modes with different axial field distributions, which can be realized by shifting the coupling position of a tapered fiber [28]. The OFCs based on degenerate FWM under anomalous dispersion, as well as Raman process in the normal dispersion regime, are observed.

II. Theoretical Analysis

The dispersion in a microbottle resonator is characterized by the variation in the azimuthal FSR$_m$ and contains two contributions: material dispersion $\Delta\nu_{\mathrm{FSR}}^{\mathrm{M}}$ and geometry dispersion $\Delta\nu_{\mathrm{FSR}}^{\mathrm{G}}$. The material dispersion originates from the variation in the material refractive index corresponding to the pump wavelength λ, and could be quantified by the group velocity dispersion (GVD) parameter [9]:

$$\Delta\nu_{\mathrm{FSR}}^{\mathrm{M}} \approx \frac{c^2\lambda^2}{4\pi^2 n^3 R_0^2}\cdot \mathrm{GVD} \tag{1}$$

where $\mathrm{GVD} = -\frac{\lambda}{c}\frac{\partial^2 n}{\partial\lambda^2}$, c is the speed of light in vacuum, n is the refractive index at a wavelength λ, which can be calculated using the Sellmeier equation, and R_0 is the maximum radius of the microbottle resonator.

On the other hand, the geometry dispersion represents the variation in the FSR$_m$ owing to the resonator geometry [9]. The resonance frequency ν_m of a fundamental bottle mode can be expressed by the following expression with the shape of the resonator considered as a harmonic profile [29]:

$$\nu_m = \frac{c}{2\pi n}\left[\left(\frac{U_m}{R_0}\right)^2 + \left(q+\frac{1}{2}\right)\Delta E_m\right]^{1/2} \tag{2}$$

where $U_m = m + \alpha(m/2)^{1/3} + (3/20)\alpha^2(m/2)^{-1/3}$, α = 2.338 is the first root of the Airy function, $\Delta E_m = 4U_m\Delta k/D$, D and Δk represent the maximum diameter and curvature of the resonator, respectively, m is the azimuthal mode number, and q is the axial mode number. Therefore, the geometry dispersion could be calculated by [9]:

$$\Delta\nu_{\mathrm{FSR}}^{\mathrm{G}} = \nu_{m+1} + \nu_{m-1} - 2\nu_m \tag{3}$$

By substituting Eq. (2) into Eq. (3), and using Eq. (1), the total dispersion $\Delta\nu_{\mathrm{FSR}}$, which contains both material dispersion and geometry dispersion, can be expressed as:

$$\Delta\nu_{\mathrm{FSR}} = \Delta\nu_{\mathrm{FSR}}^{\mathrm{M}} + \Delta\nu_{\mathrm{FSR}}^{\mathrm{G}} \tag{4}$$

The calculated total dispersion of the microbottle resonator with the axial mode number q = 0 for different pump wavelengths is shown in Figure 1(a). Two bottles (marked as sample 1 and sample 2) with different structure parameters are considered for comparison, with maximum diameters of D_1 = 166.4 μm and D_2 = 143.5 μm and bottle lengths of L_1 = 375.1 μm and L_2 = 323.6 μm, respectively. The resonator with the larger diameter has a flatter dispersion. For example, the dispersion of sample 1 varies in the range of -2.1 to 3.59 MHz at wavelengths in the range of 1.4 to 1.7 μm, while for sample 2, varies in the range of -3.43 to 3.98 MHz. The flat dispersion is beneficial for the OFC generation owing to the easy access of parametric frequency conversion [15]. Furthermore, the ZDW of sample 1 is 1527.5 nm, which is smaller than that of sample 2 (ZDW = 1557.0 nm). Figure 1(b) shows the ZDW of sample 1 as a function of the axial mode number q. Accordingly, the adjustment of the microbottle resonator ZDW can be achieved by exciting the modes with different q numbers. Specifically, the ZDW shifts from 1.53 to 1.8 μm with the variation in q from 0 to 100, revealing an effective, convenient, and wide-range ZDW adjustment approach.

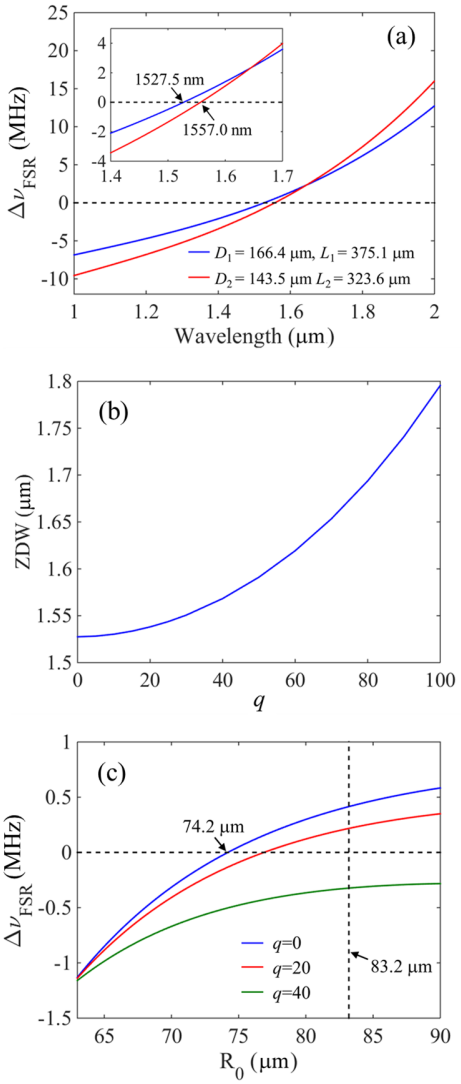

Fig. 1. (a) Total dispersion of the microbottle resonator with an axial mode number q = 0 for different incident wavelengths. The solid blue line represents sample 1 with D_1 = 166.4 μm, L_1 = 375.1 μm, while the solid red line represents sample 2 with D_2 = 143.5 μm, L_2 = 323.6 μm. (b) ZDW of sample 1 as a function of the axial mode number q. (c) Total dispersion against the maximum radius of the bottle resonator with q of 0, 20, and 40.

The relationships between the total dispersion and bottle radius for different q are shown in Figure 1(c). The total dispersion increases with the bottle diameter for a fixed q; the anomalous dispersion appears when the bottle size is larger than 74.2 μm for q=0. In addition, the dispersion distribution of the bottle mode with q = 0 is similar with that of the traditional equator mode in a microsphere resonator [23]. The vertical

This article has been accepted for publication in a future issue of this journal, but has not been fully edited. Content may change prior to final publication. Citation information: DOI 10.1109/JLT.2019.2932844, Journal of Lightwave Technology

black dashed line in Figure 1(c) corresponds to sample 1 whose maximum radius is 83.2 μm. The total dispersion of $q = 0$ is in the anomalous regime ($\Delta\nu_{FSR} > 0$), while for $q = 40$, is in the normal regime ($\Delta\nu_{FSR} < 0$), revealing the possibility to modify the dispersion sign of resonator. Experimentally, this would be easily implemented by adjusting the excitation position of the tapered fiber along the bottle axis. The tapered fiber can be positioned at the bottle center to ensure that the mode with q=0 could be excited [26]. On the other hand, the mode with $q = 40$ could be excited when the tapered fiber is moved to 51.2 μm away from the bottle center, as calculated by the axial wave function of microbottle resonator [30].

III. Experimental Results

Figure 2 illustrates the experimental setup used for the OFC generation in the microbottle resonator. Light from a tunable external cavity diode laser (ECDL, New Focus TLB-6728) in the 1550-nm band with a linewidth smaller than 200 kHz was amplified using an erbium-doped fiber amplifier (EDFA), and then launched into the microbottle resonator through a low-loss tapered fiber with waist diameter of approximately 3.5 μm. The tapered fiber was fabricated utilizing the modified flame brushing technique [31]. It was positioned perpendicular to the microbottle resonator and remained in physical contact during the experiment to provide a robust coupling and achieve a stable transmission spectrum. The microbottle resonator was fabricated by the "soften and compress" technique using a standard fusion splicer (Furukawa, Filtel S178C). A short section of a continuous single-mode fiber (Corning, SMF-28) was employed and several splicer actions were carried out on a small region to prepare a microbottle resonator [32]. Two bottles with structure parameters corresponding to sample 1 and sample 2 were prepared with different softening temperature profiles, as well as different compression distances and compression times. The intrinsic Q factors of the bottle resonators around 1550 nm were calculated to be ~ 1×10^7 by measuring the full width at half maximum (FWHM).

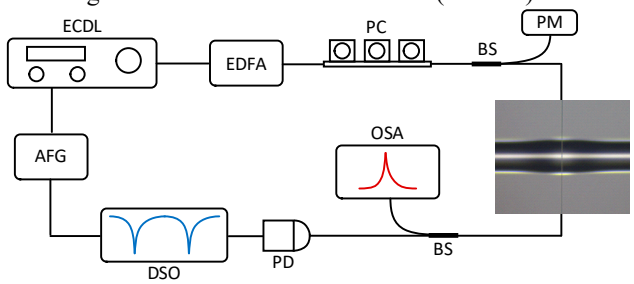

Fig. 2. Experimental setup for OFC generation in the microbottle resonator. ECDL, external cavity diode laser; EDFA, erbium-doped fiber amplifier; PC, polarization controller; BS, beam splitter; PM, power meter; OSA, optical spectrum analyzer; PD, photoelectric detector; DSO, digital sampling oscilloscope; AFG, arbitrary function generator.

A power meter (PM) was used to monitor the power incident into the resonator with the help of a 50/50 in-line beam splitter (BS). The transmission signal of the tapered fiber was divided into two paths. One path was connected to an optical spectrum analyzer (OSA, Yokogawa AQ6370D) with a resolution of 0.02 nm, while the other was monitored using an InGaAs photoelectric detector (PD, New Focus 1811), which was connected to a digital sampling oscilloscope (DSO, Agilent 4022A). The polarization state of the launched light was controlled and stabilized by a polarization controller (PC). In order to generate the OFC, the pump laser was repeatedly scanned around a high-Q WGM over 100 pm at a rate of 50 Hz using an arbitrary function generator (AFG). All experimental results were obtained with a launched pump power (the power incident into the resonaotr) of approximately 3–4 mW.

The transmission spectrum of sample 1 excited at the bottle center is shown in Figure 3. The pump wavelength of the frequency comb shown in Figure 3(a) is 1556.552 nm, while the first-order idler peak is at 1553.348 nm, with the signal at 1559.774 nm (see the inset). The first-order signal-idler photons are symmetrically distributed around the pump by 6.426 nm, which agrees with twice the azimuthal FSR_m (~ 3.210 nm) calculated by: $FSR_m = \lambda^2/2\pi nR_0$. The small difference between the observed and calculated FSRs may originate from the thermal effect and measurement error of the resonator diameter. Figures 3(b) and 3(c) show the comb spectra with 2 FSR_m and 3 FSR_m mode spacings with pump wavelengths of 1551 and 1550.8 nm, respectively. The different distances between the comb peaks originate from the modes with different radial numbers are excited simultaneously, and the energy conservation between these modes are satisfied [33]. As no Raman scattering signal is observed, the frequency combs in Figure 3 could be attributed to the degenerate FWM in which the two pump photons have the same frequency. All of the pump wavelengths in Figure 3 are larger than the ZDW of sample 1, corresponding to the mode dispersion in the anomalous regime with $q = 0$ (shown in Figure 1(a)).

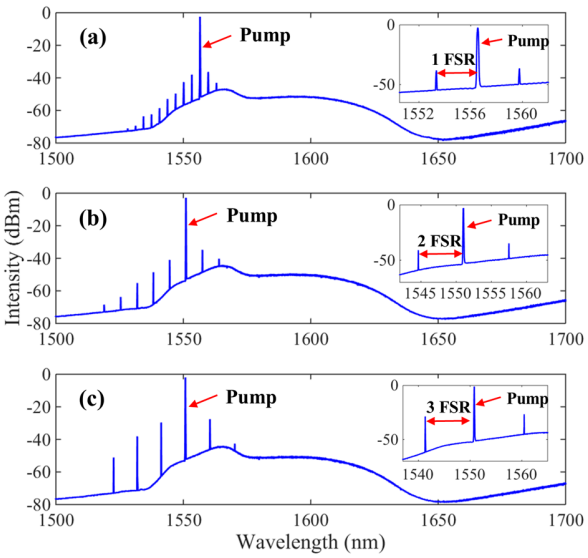

Fig. 3. Transmitted spectra of sample 1 with pump wavelengths of a 1556.5, b 1551, and c 1550.8 nm. The tapered fiber is positioned at the bottle center.

The transmitted optical spectrum of sample 2 with $q = 0$ is then investigated under anomalous dispersion, i.e., with a pump wavelength larger than 1556.9 nm, according to Figure 1(a). The spectra shown in Figures 4(a) and 4(b) illustrate the OFC

This article has been accepted for publication in a future issue of this journal, but has not been fully edited. Content may change prior to final publication. Citation information: DOI 10.1109/JLT.2019.2932844, Journal of Lightwave Technology

generations of sample 2 pumped at 1567.7 and 1558.2 nm, respectively. In addition to the frequency comb with an interval of 1 FSR$_m$ shown in Figure 4(a), a comb spaced by 1/4 FSR$_m$ is also generated (see Figure 4(b)), as the azimuthal FSR$_m$ (~3.69 nm) of the bottle resonator is exactly four times larger than the axial $\mathrm{FSR}_q = \lambda^2 \Delta k / 2\pi n \approx 0.923\mathrm{nm}$ [34], which has been theoretically predicted in Ref. [35]. Furthermore, the comb peaks with the 5/4 FSR$_m$ mode spacing (green arrows) are higher than the adjacent peaks. This could be explained as combs with a 5/4 FSR$_m$ mode spacing are generated, and then with the help of a cascaded nondegenerate FWM, the subsequent comb peaks with the 1/4 FSR$_m$ mode spacing are efficiently generated [15].

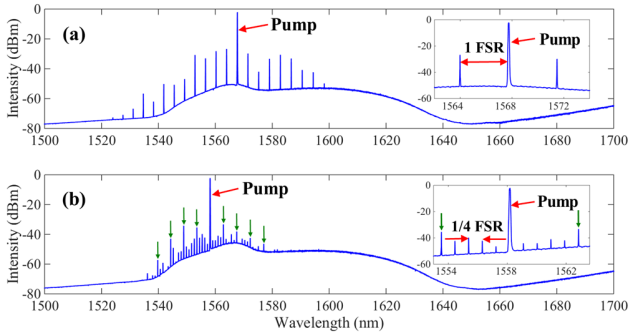

Fig. 4. Transmitted spectra of sample 2 with pump wavelengths of (a) 1567.7 and (b) 1558.2 nm. The tapered fiber is positioned at the bottle center.

In order to demonstrate the ZDW adjustment based on the coupling position, the tapered fiber was moved to 51.2 μm away from the bottle center of sample 1, as mentioned above. This position was measured with the help of a charge-coupled device (CCD) camera above the coupling regime and the obtained spectrum is shown in Figure 5(a). The peak centered at 1656.3 nm shown in Figure 5(a) corresponds to the stimulated Raman scattering (SRS), down-shifted by approximately 12.4 THz relative to the pump mode. SRS is a pure gain process where a photon is red-shifted and creates an optical phonon. It is worth noting that no FWM was observed in this case even at a decreased pump power below the Raman threshold, which demonstrates a convenient and simple method for ZDW adjustment.

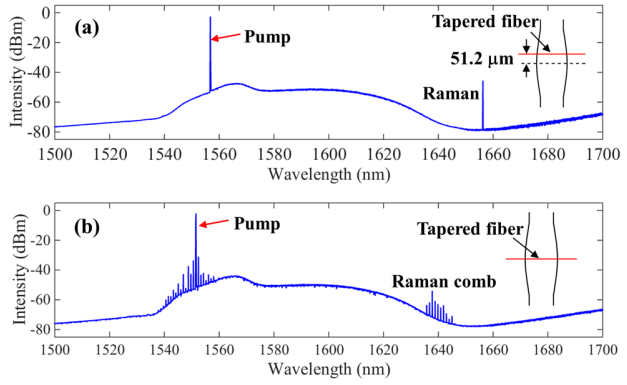

Fig. 5. (a) Transmitted spectrum of sample 1 with a pump wavelength of 1556.8 nm when the tapered fiber is positioned 51.2 μm away from the bottle center (see the inset on the right). (b) Transmitted spectrum of sample 2 with a pump wavelength of 1551.5 nm when the tapered fiber is positioned at the bottle center.

In addition to the ZDW control based on the excitation position, the dispersion sign could also be changed by tuning the pump wavelength, as shown in Figure 1(a). For sample 2, the normal dispersion of the mode with $q = 0$ could be realized by adjusting the pump wavelength smaller than 1556.9 nm. Figure 5(b) shows the spectrum generated at a wavelength of 1551.5 nm. Two distinct spectral regions can be distinguished: a Raman comb constituted of SRS family modes and Raman-assisted comb in the vicinity of the pump with an identical spacing of 1/4 FSR$_m$. This comb spectrum is generated initially by a Raman scattering, which down-shifts its frequency, followed by nondegenerate FWM processes in which all four photons have different frequencies [36]. The Raman and Raman-assisted OFCs observed in Figure 5(b) provide a broadened spectrum toward the longer wavelengths, and indicate that the frequency comb based on the degenerated FWM requires anomalous dispersion. However, the selectable dispersion based on pump wavelength is restricted by the operating wavelength of the laser.

IV. Conclusion

The FWM and OFC generation in the WGM microbottle resonator were investigated. The ZDW of the bottle resonator was effectively adjusted by changing the coupling position of the tapered fiber. The degenerated FWM-based OFC, as well as Raman-assisted OFC, were observed by pumping the bottle resonator in different dispersion regimes. Additionally, the OFC with a sideband spacing of 1/4 FSR$_m$ was generated when the azimuthal FSR$_m$ of the bottle resonator was exactly four times larger than the axial FSR$_q$. The ZDW adjustment method proposed in this paper is convenient and simple for WGM microresonators. This study could facilitate the research on OFC generation in the telecom and mid-infrared regimes.

References

[1] F. Adler, M. J. Thorpe, K. C. Cossel, J. Ye, "Cavity-enhanced direct frequency comb spectroscopy: technology and applications," *Annu. Rev. Anal. Chem.*, vol. 3, pp. 175–205, Mar. 2010.

[2] T. Udem, R. Holzwarth, T. W. Hänsch, "Optical frequency metrology," *Nature*, vol. 416, no. 6877, pp. 233–237, Mar. 2002.

[3] J. Ye, H. Schnatz, L. W. Hollberg, "Optical frequency combs: from frequency metrology to optical phase control," *IEEE Journal of Selected Topics in Quantum Electronics*, vol.9, no. 4, pp.1041–1058, Jul. 2003.

[4] T. M. Fortier, M. S. Kirchner, F. Quinlan, J. Taylor, J. C. Bergquist, T. Rosenband, N. Lemke, A. Ludlow, Y. Jiang, C. W. Oates, S. A. Diddams, "Generation of ultra-stable microwaves via optical frequency division, " *Nature Photon.*, vol. 5, no. 7, pp. 425–429, Jul. 2011.

[5] V. R. Supradeepa, C. M. Long, R. Wu, "Comb-based radiofrequency photonic filters with rapid tunability and high selectivity," *Nature Photon.*, vol. 6, no. 3, pp. 186–194, Mar. 2012.

[6] D. Hillerkuss, R. Schmogrow, T. Schellinger, D. Hillerkuss, R. Schmogrow, T. Schellinger, M. Jordan, M. Winter, G. Huber, T. Vallaitis, R. Bonk, P. Kleinow, F. Frey, M. Roeger, S. Koenig, A. Ludwig, A. Marculescu, J. Li, M. Hoh, M. Dreschmann, J. Meyer, S Ben Ezra, N. Narkiss, B. Nebendahl, F. Parmigiani, P. Petropoulos, B. Resan, A. Oehler, K. Weingarten, T. Ellermeyer, J. Lutz, M. Moeller, M. Huebner, J. Becker, C. Koos, W. Freude, J. Leuthold, "26 Tbit s-1 line-rate super-channel transmission utilizing all-optical fast Fourier transform processing," *Nature Photon.*, vol. 5, no. 6, pp. 364–371, Jun. 2011.

[7] J. Pfeifle, V. Brasch, M. Lauermann, Y. M. Yu, D. Wegner, T. Herr, K. Hartinger, P. Schindler, J. S. Li, D. Hillerkuss, R. Schmogrow, C.

Weimann, R. Holzwarth, W. Freude, J. Leuthold, T. J. Kippenberg, C. Koos, "Coherent terabit communications with microresonator Kerr frequency combs," *Nature Photon.*, vol. 8, no. 6, pp. 375–380, Jun. 2014.

[8] K. J. Vahala, "Optical microcavities," *Nature*, vol. 424, no. 6950, pp. 839–846, Aug. 2003.

[9] P. Del'Haye, A. Schliesser, O. Arcizet, T. Wilken, R. Holzwarth, T. J. Kippenberg, " Optical frequency comb generation from a monolithic microresonator," *Nature*, vol. 450, no. 7173, pp. 1214-1217, Dec. 2007.

[10] Y. Yang, X. F. Jiang, S. Kasumie, G. M. Zhao, L. H. Xu, J. M. Ward, L. Yang, S. N. Chormaic, " Four-wave mixing parametric oscillation and frequency comb generation at visible wavelengths in a silica microbubble resonator," *Opt. Lett*., vol. 41, no. 22, pp. 5266-5269, Nov. 2016.

[11] S. V. Suchkov, M. Sumetsky, and A. A. Sukhorukov, "Frequency comb generation in SNAP bottle resonators", *Opt. Lett.*, vol. 42, no. 11, pp. 2149-2152, Jun. 2017.

[12] G. P. Lin, S. Diallo, J. M. Dudley, and Y. K. Chembo, "Universal nonlinear scattering in ultra-high Q whispering gallery-mode resonators," *Opt. Express*, vol. 24, no. 13, pp. 14880-14894, Jun. 2016

[13] P. Parra-Rivas, D. Gomila, M. A. Matias, S. Coen, and L. Gelens, "Dynamics of localized and patterned structures in the Lugiato-Lefever equation determine the stability and shape of optical frequency combs," *Phys. Rev. A*, vol. 89, no. 4, pp. 043813, Apr. 2014.

[14] T. J. Kippenberg, R. Holzwarth, S. A. Diddams, " Microresonator-based optical frequency combs," *Science*, vol. 332, no. 6029, pp. 555-559, Apr. 2011

[15] C. L. Guo, K. J. Che, H. Y. Xu, P. Zhang, D. Y. Tang, C. Y. Ren, Z. Q. Luo, Z. P. Cai, "Generation of optical frequency combs in a fiber-ring/microresonator laser system," *Opt. Lett*., vol. 41, no. 11, pp. 2576-2579, Jun. 2016.

[16] T. J. Kippenberg, S. M. Spillane, K. J. Vahala, "Kerr-nonlinearity optical parametric oscillation in an ultrahigh-Q toroid microcavity," Phys. *Rev. Lett*., vol. 93, no. 8, pp. 083904, Aug. 2004.

[17] I. H. Agha, Y. Okawachi, A. L. Gaeta, "Theoretical and experimental investigation of broadband cascaded four-wave mixing in high-Q microspheres," *Opt. Express*, vol. 17, no. 18, pp. 16209–16215, Aug. 2009.

[18] X. X. Xue, M. H. Qi, A. M. Weiner, " Normal-dispersion microresonator Kerr frequency combs," *Nanophotonics*, vol. 5, no. 2, pp. 244-262, Jun. 2016.

[19] I. H. Agha, Y. Okawachi, M. A. Foster, J. E. Sharping, A. L. Gaeta, " Four-wave-mixing parametric oscillations in dispersion-compensated high-Q silica microspheres," *Phys. Rev. A*, vol. 76, no. 4, pp. 043837, Oct. 2007.

[20] D. Farnesi, A. Barucci, G. C. Righini, G. N. Conti, S. Soria, "Generation of hyper-parametric oscillations in silica microbubbles," *Opt. Lett.,* vol. 40, no. 19, pp. 4508, Oct. 2015.

[21] N. Riesen, W. Q. Zhang, T. M. Monro, "Dispersion analysis of whispering gallery mode microbubble resonators," *Opt. Express*, vol. 24, no. 8, pp. 8832, Apr. 2016.

[22] N. Riesen, W. Q. Zhang, T. M. Monro, "Dispersion in silica microbubble resonators," *Opt. Lett.*, vol. 41, no. 6, pp. 1257, Mar. 2016.

[23] M. Li, X. Wu, L. Y. Liu, L. Xu, "Kerr parametric oscillations and frequency comb generation from dispersion compensated silica micro-bubble resonators," *Opt. Express*, vol. 21, no.14, pp. 16908, Jul. 2013.

[24] J. M. Ward, S. Nic Chormaic, "Thermo-optical tuning of whispering gallery modes in Er: Yb co-doped phosphate glass microspheres," *Appl. Phys. B*, vol. 100, no. 4, pp. 847-850, Sep. 2010.

[25] R. Henze, T. Seifert, J. Ward, O. Benson, "Tuning whispering gallery modes using internal aerostatic pressure," *Opt. Lett*., vol. 36, no. 23, pp. 4536–4538, Dec. 2011.

[26] Y. H Yin, Y. X. Niu, M. X. Ren, W. Wu, W. S. Zhao, J. Nan, Z. Y. Zheng, Y. Zhang, M. Ding, "Strain sensing based on a microbottle resonator with cleaned-up spectrum," *Opt. Lett*., vol. 43, no. 19, pp. 4715-4718, Oct. 2018.

[27] S. V. Suchkov, M. Sumetsky and A. A. Sukhorukov, Frequency comb generation in SNAP bottle resonators, vol. 42, no. 11, *Opt. Lett.*, pp. 2149-2152, Jun. 2017

[28] Y. H. Yin, Y. X. Niu, L. L. Dai, M. Ding, "Cascaded microbottle resonator and its application in add–drop filter," *IEEE Photonics J.*, vol. 10, no. 4, pp.1, Aug. 2018.

[29] G. S. Murugan, M. N. Petrovich, Y. Jung, J. S. Wilkinson, M. N. Zervas, "Hollow-bottle optical microresonators," *Opt. Express*, vol. 19, no. 21, pp. 20773-20784, Oct. 2011.

[30] Y. Louyer, D. Meschede, and A. Rauschenbeutel, "Tunable whispering-gallery-mode resonators for cavity quantum electrodynamics", *Phys. Rev. A*, vol. 72, no. 3, pp. 031801, Sep. 2005

[31] G. Brambilla, F. Koizumi, X. Feng, D. J. Richardson, "Compound-glass optical nanowires," *Electron. Lett*., vol. 41, no. 7, pp. 400-402, Mar. 2005.

[32] G. S. Murugan, J. S. Wilkinson, M. N. Zervas, "Selective excitation of whispering gallery modes in a novel bottle microresonator," *Opt. Express*, vol. 17, no. 14, pp. 11916–11925, Jul. 2009.

[33] G. P. Lin, Y. K. Chembo, "On the dispersion management of fluorite whispering-gallery mode resonators for Kerr optical frequency comb generation in the telecom and mid-infrared range," *Opt. Express*, vol. 23, no. 2, pp. 1594-1604, Jan. 2015.

[34] A. A. Savchenkov, A. B. Matsko, W. Liang, V. S. Ilchenko, D. Seidel and L. Maleki, Kerr combs with selectable central frequency, *Nat. Photonics*, vol. 5, pp. 293-296, May 2011.

[35] V. Dvoyrin and M. Sumetsky, Bottle microresonator broadband and low-repetition-rate frequency comb generator, *Opt. Lett.*, vol. 41, no. 23, pp. 5547-5550, Dec. 2016.

[36] G. P. Lin, and Y. K. Chenbo, "Phase-locking transition in Raman combs generated with whispering gallery mode resonators," *Opt. Lett.*, vol. 41, no. 16, pp. 3718-3721, Aug. 2016.

Yiheng Yin received the M.S. degree in applied physics from Shandong University of Science and Technology, Qingdao, China, in 2014. He is currently working toward the Ph.D. Degree at the School of Instrumentation Science and Optoelectronic Engineering, Beihang University, Beijing, China. His current research interests include fiber–coupled microresonators, surface plasmon polaritons, and add -drop filters.

Yanxiong Niu received the bachelor's degree in Physics from Xuzhou Normal University, Xuzhou, China, in 1989, the master's degree in Military Photoelectric from National University of Defense Technology, Changsha, China, in 1992, and the PhD's degree in Physical Electronics from Tianjin University, Tianjin, China, in 2005. He is currently a Professor with School of Instrumentation Science and Opto -Electronics Engineering, Beihang University, Beijing, China. His current research interests include fiber -coupled microresonators and the design of optoelectronic system.

Haoye Qin is currently pursuing the bachelor's degree in Instrumentation Science and Technology, Beihang University, Beijing, China. His main research interests include the micro/nano fiber sensing and applications based on whispering gallery mode microbottle resonator.

Ming Ding received the B.Sc. (Hons.) degree in optical information science and technology from Beijing Jiaotong University, China and the Ph.D. degree in optoelectronics from the Optical Fiber Nanowires and Related Devices Group, Optoelectronics Research Centre, University of Southampton, Southampton, U.K. She is currently a Professor with School of Instrumentation Science and Opto-Electronics Engineering, Beihang University, Beijing, China. Her current research interests include optical fiber sensors, quantum sensor, micro - and nanoresonators, micro - and nanofiber.